Journal of Power Sources 185 (2008) 1465–1470

Contents lists available at ScienceDirect

Journal of Power Sources

journal homepage: www.elsevier.com/locate/jpowsour

Determination of new time–temperature-transformation diagrams for lead–calcium alloys

F. Rossi [a,*], M. Lambertin [a], L. Delfaut-Durut [b], A. Maitre [c], M. Vilasi [d]

[a] Arts et Métiers Paristech, LaBoMaP, ENSAM, Rue porte de Paris, 71250 Cluny, France
[b] CEA, centre de Valduc [SEMP, LECM], 21120 Is-sur-Tille, France
[c] SPCTS, UFR Sciences et techniques, 87060 Limoges, France
[d] LCSM, Université Nancy I, 54506 Vandoeuvre les Nancy, France

ARTICLE INFO

Article history:
Received 10 July 2008
Received in revised form 8 September 2008
Accepted 10 September 2008
Available online 18 September 2008

Keywords:
Lead alloys
Ageing
Time–temperature-transformation diagrams
Kinetics
Micro-hardness
Resistivity

ABSTRACT

The Pb–Ca is an age hardening alloy that allows for an increase in the hardness compared to pure lead. The hardening is obtained after different successive ageing transformations. In addition, this hardening is followed by an overageing which induces a softening.

The ageing and overageing transformation mechanisms are now well identified in lead–calcium alloys. In this paper, we propose to represent the domain of stability of each transformation via time–temperature-transformation diagrams for a calcium concentration from 600 to 1280 ppm and in a range of temperatures from −20 to 180 °C. These diagrams are constructed with the data obtained by in situ ageing with metallographic observations, hardness and electrical resistance measurements. The specificities of lead–calcium such as its fast ageing at ambient temperature and its overageing over time required the design of specific devices to be able to identify the characteristics of these alloys.

1. Introduction

Lead–calcium alloys are widely used, mainly in the automotive industry in grids battery to cope with the softness and the low creep resistance of pure lead. Calcium allows for a significant improvement in the mechanical properties by a precipitation hardening from an oversaturated α solid solution. Room temperature ageing corresponds to a continuous annealing treatment, so after a hardening stage, the alloy will progressively lose its properties by overageing. Over the last 70 years, much research has been carried out to identify the transformations occurring in these alloys [1–4]. Now the transformations occurring in lead–calcium alloys are clearly identified with three successive hardening transformations and the two softening ones. It is necessary to determine accurately the kinetics of these transformations to be able to predict the ageing of alloys or to determine heat treatments to achieve a given microstructural state.

2. Experiments

2.1. Alloys preparation

The samples have calcium levels around the peritectic point (0.08 wt%Ca). Alloys are obtained by mixing industrial lead–calcium alloys (calcium content 0.108 wt%) with "pure" lead (99.97 wt%). The chemical compositions measured by inductive coupled plasma-mass spectrometry (ICP-MS) and inductive coupled plasma-atomic emission spectroscopy (ICP-AES) are summarized in Table 1.

The alloy is melted in a crucible at 600 °C in a protective atmosphere. The samples are obtained by casting and their shapes are adapted to the technique of characterisation. For the measurements of resistance, very long samples are used (2 mm × 3 mm × 100 mm) in order to maximise the electrical signal (Fig. 1). Hardness measurements and metallographic observations are performed on samples (9 mm × 9 mm × 13 mm) sawn from much larger plates (13 mm × 120 mm × 120 mm) (Fig. 2). To enable significant hardening during ageing, the alloy for resistance measurements is cast in a cold mould and so quenched from the liquid state in order to obtain an oversaturated solid solution at room temperature. Alloy used for hardness measurements is cast in a preheated mould and quenched with the mould as it is still in liquid state. These opera-

* Corresponding author. Tel.: +33 3 85 59 51 13; fax: +33 3 85 59 53 70.
E-mail address: rossi@cluny.ensam.fr (F. Rossi).

0378-7753/$ – see front matter © 2008 Elsevier B.V. All rights reserved.
doi:10.1016/j.jpowsour.2008.09.023

Table 1
Chemical composition of the used alloys measured by inductive coupled plasma-mass spectrometry (ICP-MS) and inductive coupled plasma-atomic emission spectroscopy (ICP-AES).

Chemical composition (wt ppm)	Ca	Al	Sn	Bi	Mg	Ag	Ni	Cu	Sb	As	Zn	Cd	Pb
Pb–Ca alloy (METALEUROP)	1080	161	1	130	/	36	1	4	1	1	3	1	–
Pure lead (BUDIN et Fils)	/	/	3	250	/	10	/	10	3	2	10	3	–
Pb–0.06 wt%Ca	593	31	17	50	2	22	4	3	<1	<1	<1	<1	–
Pb–0.1 wt%Ca	1027	67	13	89	2	33	6	4	<1	<1	<1	<1	–

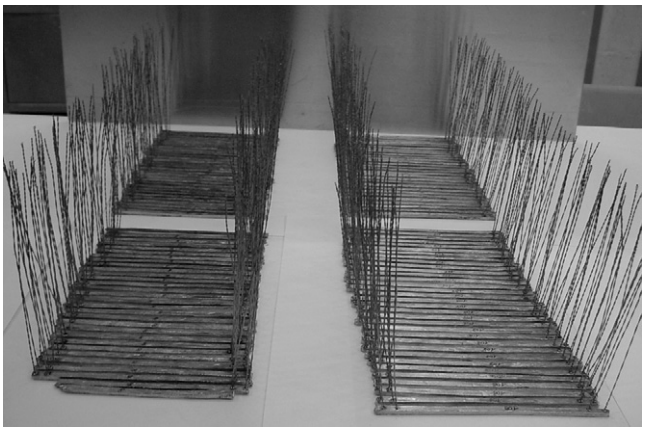

Fig. 1. Samples used for the resistance measurements with the spark welded copper probes for the four-point method measurements.

tions of quenching directly after casting avoid a further annealing. The cooling speed is around −50 to −100° s^{-1}. After complete cooling, the mould with the part is immediately immersed in liquid nitrogen in order to stop the first precipitation transformations. Further sampling and preparation will be performed in liquid nitrogen, or possibly for short times at temperatures under −50 °C.

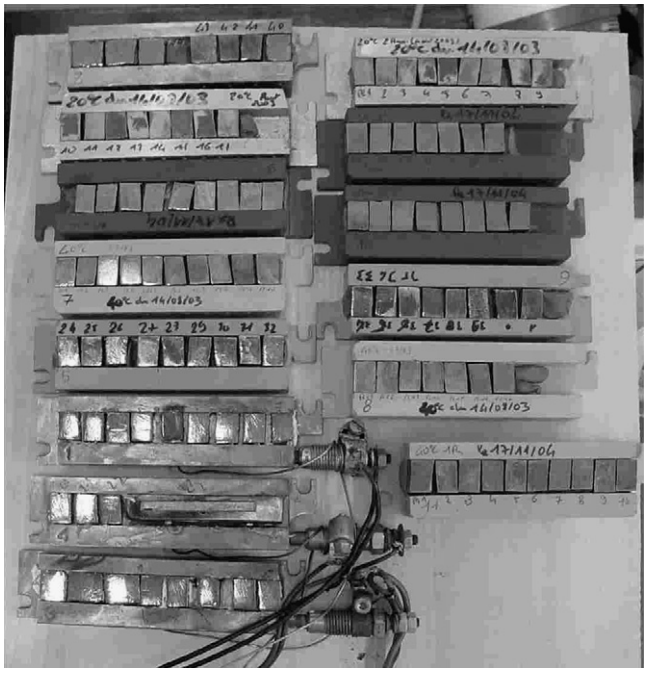

Fig. 2. Samples used for the micro-hardness measurements on their thermoregulated mounting.

2.2. Resistance measurements

Resistance measurements have been widely used to identify the kinetics of lead alloy transformations [2,5–9] with its sensitivity to atomic defects, and more precisely to the elements in solid solution. For oversaturated lead–calcium alloys, it is then possible to identify the first transformations by monitoring the electrical resistance in relation to time in isothermal conditions. The four-point method was used with samples 100-mm long and a section of 2 mm × 3 mm. The copper probes are spark welded in line on the sample extremities while the sample is kept in liquid nitrogen. The measurements are performed on a specially designed piece of experimental equipment which enable us to control the annealing treatment temperature in three oil baths from −20 to 275 °C with a temperature stability of 0.1 °C. The entire experiment is fully automated with measurement accuracy of less than 0.1% of the signal magnitude (Fig. 3). The full automation of the measurements has enabled to characterise 120 samples and to record more than 2,500,000 measurements on a cumulated time of more than 20 years.

2.3. Micro-hardness measurements

The first two transformations occurring in lead–calcium alloys are of discontinuous type, thus it is necessary to have punctual information of the evolution of the alloy. Micro-hardness was used to be able to identify the characteristics of the mean of the hardness and the heterogeneity of the sample (Fig. 3). Measurements were taken on thermoregulated samples (from 20 to 80 °C), in situ with a specific redesigned micro-hardness tester. A 10 N load was applied for 5 s with a micro-Vickers hardness tester LECO AMH2000. The samples were electrochemically polished at −50 °C to prevent any microstructural transformations before the test. Hardness measurements were performed on 50 samples over 2 years (more

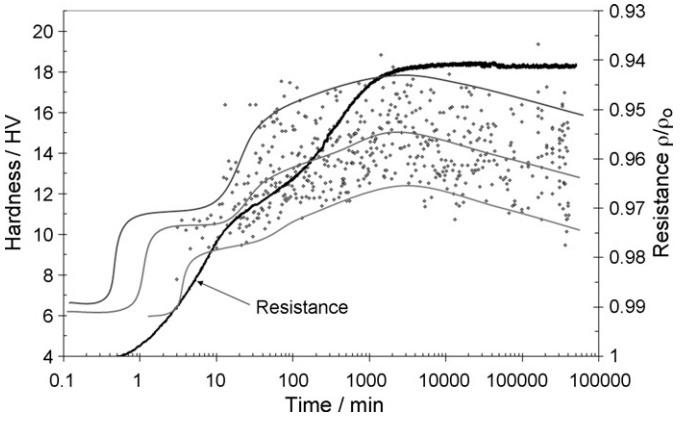

Fig. 3. Typical micro-hardness and resistance curves for a Pb–0.1 wt% at 20 °C. In black the value of the resistance over the resistance at initial time (oversaturated alloy). The points correspond to hardness measurements $HV_{0.1/5}$ on a single sample. As samples are inhomogeneous in hardness due to the presence of discontinuous transformations, fitted grey solid lines are added to represent the mean and the maximum, minimum curve to visualise the hardness amplitude.

than 80,000 indentations with a cumulated time of more than 100 years). All these data have been used to construct new TTT diagrams for lead–calcium alloys.

3. Results

3.1. Lead alloy containing 1000 ppm of calcium

3.1.1. Time–temperature-transformation diagram

The law of transformation at room temperature of an alloy in non-equilibrium conditions is not sufficient to overcome its metallurgical evolution. It is necessary to have several transformation curves in isothermal conditions, staggered in all the range of instability of the alloy. It will then be possible to define with precision the heat treatment (temperature and duration) needed for the alloy to be in a given metallurgical state. It will also allow us to predict the metallurgical state of an alloy if its thermal background (ageing time and temperature) is known. The entire experimental results are summarized together in time–temperature-transformation diagrams. The TTT diagram is established with the start and finish times of each transformation during isothermal treatment. The domains of transformation of the alloy Pb–0.1 wt%Ca have been precisely defined by the kinetics of transformation determined by hardness and electrical resistance measurements and by the metallographic and transmission electron microscope (TEM) observations. Its TTT diagram is shown in Fig. 4.

In the first few minutes after the quench (oversatured calcium state), the alloy exhibits a homogeneous hardness of 6 $HV_{/0.1/5}$, up to the beginning of the first discontinuous transformation. The curve C_1 (Fig. 4) represents the time which is needed to obtain a transformation rate of around 10% of the first transformation. It means that the transformation (initiated between the grains boundaries) does start before C_1, otherwise nearly immediately after the quench. This early beginning of the transformation is confirmed by the observation by optical metallography of a transformation front in the first few seconds of ageing after an electrochemical polishing and etching preparation at −50 °C (Fig. 5). For the mechanical properties, curve C_1 (the first transformation) corresponds to the first increase in hardness (Fig. 3 for example).

The second transformation, named "puzzling" because of its distinctive erratic shape of transformation fronts, appears before the end of the first transformation. Curve C_2 is thus the limit corresponding to the time when the second transformation becomes predominant to the first one. This curve corresponds to a hardness of 11 $HV_{/0.1/5}$, i.e. the end of the first increase in hardness. Our observations show that a calcium concentration, in a range of 600–1000 ppm, has no effect on these hardness values.

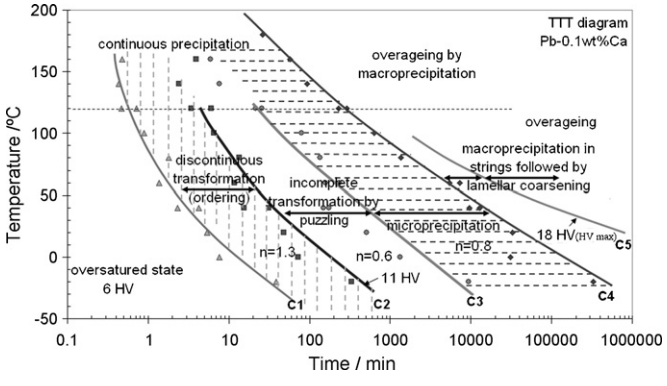

Fig. 4. TTT diagram for the alloy Pb–0.1 wt%Ca. Samples were cast, then cooled in liquid state at a minimum of 40 °C s^{-1} to −196 °C. Curves are obtained by resistivity and hardness measurements performed in a subsequent in situ heat treatments carried out in the temperature range −20 to 180 °C. The solid lines through the data points are curve fits.

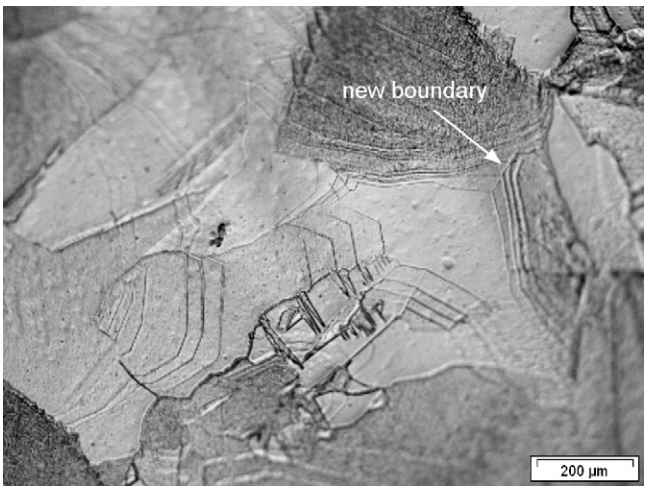

Fig. 5. Metallographic observation of a recrystallised Pb–0.1 wt%Ca alloy, annealed and quench at 100 °C s^{-1} to −196 °C. Sample is prepared by electrochemical polishing at −50 °C. Four etchings are performed at −50 °C every 3 min of ageing at 20 °C. The successive position of the advancement fronts (separating transformed and not yet transformed zones) are then visible on the same picture with notably the formation of new boundary formed by the meeting of moving fronts.

Curve C_3 defines the beginning of the microprecipitation of calcium with the formation of precipitates Pb_3Ca with a size of 2–3 nm. Curve C_4 corresponds to the completion of this precipitation with a progression rate of 90%. After this curve, the resistivity measurements will no longer evolve because all the calcium has been consumed by the precipitates and its level in solid solution will be fixed during the coarsening of the precipitates. Only the hardness measurements or the optical and TEM observations will be able to follow the alloy overageing (Fig. 6).

Curve C_5 specifies the time required to reach the maximum hardness of the alloy. Over this curve, the hardnesss will decrease gradually. C_5 has shifted from C_4 because at C_4 the microprecipitation is not completely finished and the macro-reprecipitation in strings will need some time to have a softening effect [10]. The ultimate overageing will be caused by the appearance of lamellar precipitates formed by the coalescence of the strings of macroprecipitates (Fig. 7).

Above 120 °C, the ageing mechanisms are changed to a unique and continuous macroprecipitation. The overageing will not let lamellar precipitates appear, but only isolated macroprecipitates.

Lead–calcium alloys are known to be sensitive to ternary elements [2] most of the time present as impurities of secondary metallurgy from recycled alloys from batteries (Sn, Bi, Ag, Sb, etc.) or sometimes voluntary added like aluminium to prevent oxidation in liquid phase. Small amount of these elements may have a significant impact on alloys ageing as it was described by Bourguignon in the cast of Pb–Ca–Sn alloys [8]. She has showed that discontinuous transformations which are initiated in the grain boundaries (where tin is segregated during solidification) are slowed down or even completely inhibited. Slightly different chemical composition of the one used (Table 1) to establish our TTT diagrams (Figs. 4, 10, 11, 13, 8) may modify partially the position of the domains.

Process can affect ageing: complementary studies have shown that the sole significant process parameter is the quenching speed [10]. If alloys are quenched too slowly, the first discontinuous trans-

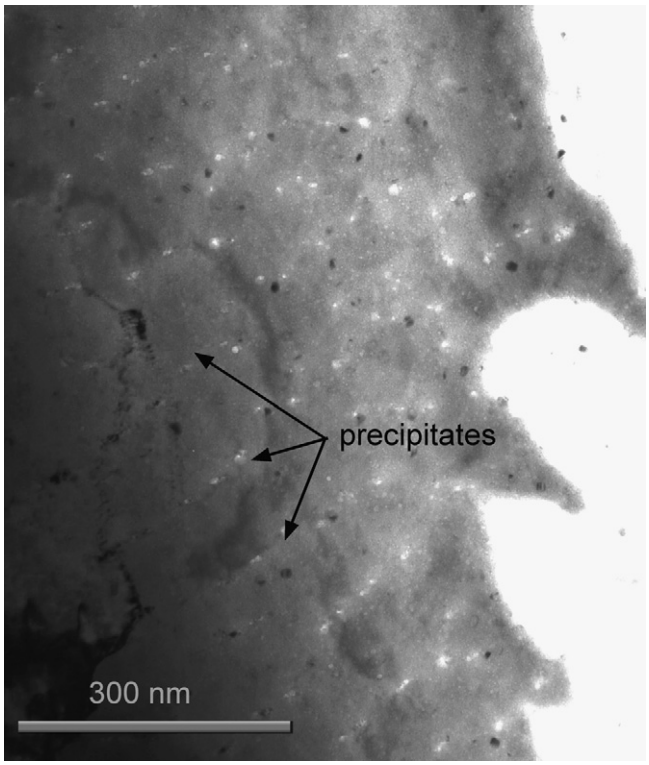

Fig. 6. TEM picture of the coarsening precipitates after 35 h of ageing at 80 °C on a Pb–0.1 wt% Ca alloy. Precipitate of Pb_3Ca are visible in white and are aligned in strings in the lead matrix.

formation occurs at high temperatures (during the cooling) and affects strongly the kinetics and the completion of the transformations. Alloys used in our study are quenched at rates of 120 °C s^{-1} for the resistivity samples and 40 °C s^{-1} for the other samples. Our TTT diagrams are only valid if the cooled rate is higher than the critical quenching speed (10 °C s^{-1} for a Pb–0.1 wt%Ca).

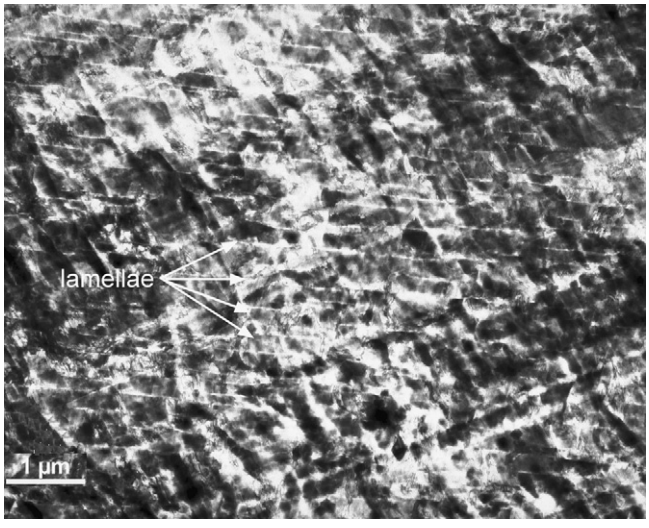

Fig. 7. TEM picture of the lamellae precipitates on an overaged lead–calcium alloy aged 120 months at room temperature. The size of the overaged zone is about 40 µm. Lamellae are formed by the coarsening of the macroprecipitates aligned in strings. Undulations oriented around 30° to the lamellae are deformations cause by the ultramicrotomy cut of the specimen. The white stain have been analysed by energy electron loss spectrometry (EELS) and are oxides formed during the observations of the specimen under the electron beam.

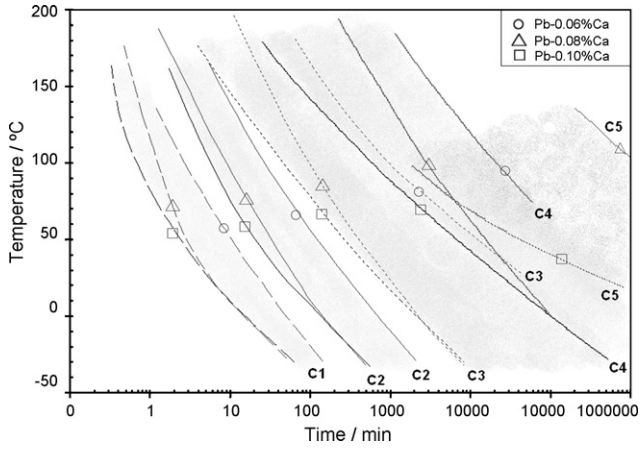

Fig. 8. TTT diagram for the concentrations of calcium of 600, 800 and 1000 ppm. Samples were cast, then cooled in liquid state at a minimum of 40 °C s^{-1} to −196 °C. Curves are obtained by resistivity and hardness measurements performed in a subsequent in situ heat treatments carried out in the temperature range −20 °C to 180 °C. The solid lines through the data points are curve fits.

3.1.2. Transformation kinetics

It is possible to calculate the apparent activation energy of each transformation from the kinetics of transformations. The transformations kinetics have been modelled by the equation of Johnson–Mehl–Avrami [11] (Eq. (1)). This expression is also applicable for discontinuous transformations. The coefficient k is thermally activated and is defined by the Arrhenius equation (Eq. (2)):

$$f = 1 - \exp(-kt^n) \quad (1)$$

with t length of ageing (s); k, n constants; f rate of transformation defined for example with resistance measurement by $f = \rho_o - \rho_f / \rho_o - \rho_f$ with ρ_o initial value of the resistance (Ω m), ρ_f final value of the resistance (Ω m).

$$k = k_0 \exp\left(\frac{-Q}{RT}\right) \quad (2)$$

with k_0 constant; Q apparent activation energy of the transformation (J mol^{-1}); T the temperature (K); R Boltzman constant (8.14 J mol^{-1} K^{-1}).

The slopes obtained by the drawing of the logarithm of the start and finish times of transformations versus the temperature enable us to find the apparent activation constant (Fig. 9). The activation energy varies between 18 and 35 kJ mol^{-1} for an alloy Pb–0.1 wt%Ca. The values are non-temperature sensitive and are lower than the autodiffusion of lead which is around 110 kJ mol^{-1} [12,13]. Our values are close to those already found in other papers. For example, Tsubakino et al. [6] has calculated activation energy of 21 and 60 kJ mol^{-1} for the first and the third transformation. These values may be interesting to compare with the parameters of the diffusion of the calcium in lead, but these data are not available.

3.2. Effect of the calcium amount

The established TTT diagram enables us to define the treatment conditions necessary to obtain a given microstructural (mechanical) state or to predict the state of an alloy from its ageing parameters. The diagram shown in Fig. 4 corresponds to the evolution of a Pb–0.1%pdsCa alloy. Industrially, calcium is used with a large range of concentrations from 400 to 1000 ppm and the sensitivity to oxidation of calcium during the preparation of the alloy by casting can produce significant loss if it is not properly protected by the addition of aluminium. Concentration of calcium has a pre-

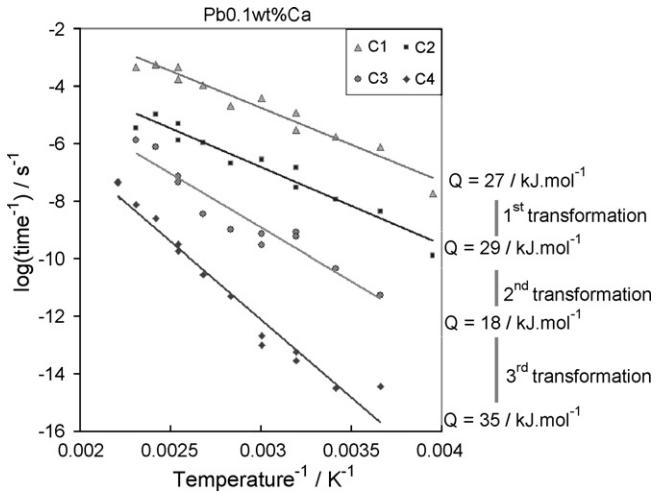

Fig. 9. Draw of the Arrhenius law for transformations of an alloy Pb–0.1 wt%Ca, calculated from the data of the TTT diagram curves.

dominant effect on the kinetics of transformations [2] and one of the consequences is the modification of the position of the limits of the TTT diagram. Several diagrams for different calcium levels have been plotted to quantify this parameter.

3.2.1. Hypoperitectic compositions (600 ppm Ca)

The kinetics of transformations are significantly lower for a Pb–0.06 wt%Ca alloy than for concentrations of 1000 wt ppm of calcium. The curves of the TTT diagram are consequently shifted to the right (Fig. 10) with hardness levels slightly lower (0.3 HV) during ageing. For the Pb–0.1 wt%Ca alloy, the curve C_1 corresponds to the first increase in hardness, whereas for concentration of 600 wt ppm, the beginning of the hardening occurs after C_1. The first hardening ends at curve C_2 with a mean hardness of 10.6 $HV_{/0.1/5}$. At room temperature, it is not easy to see the overageing which will occur after several years. For ageing temperatures, over 120 °C, the ageing is done by a single and continuous macroprecipitation of Pb_3Ca.

3.2.2. Peritectic compositions (800 ppm Ca)

Alloys of composition Pb–0.08 wt%Ca are particularly important because it is the most common composition used industrially.

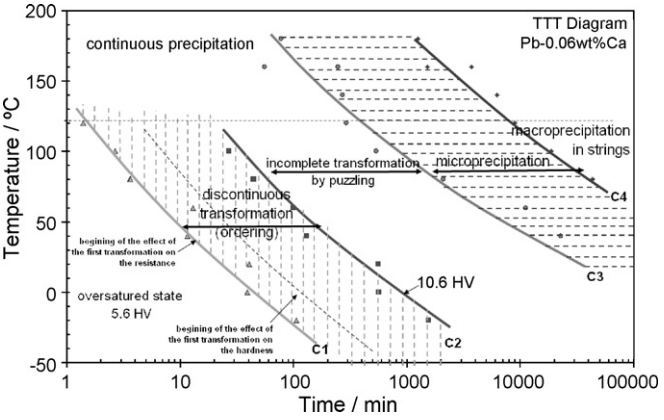

Fig. 10. TTT diagram of an alloy Pb–0.06 wt%Ca. Samples were cast, then cooled in liquid state at a minimum of 40 °C s^{-1} to −196 °C. Curves are obtained by resistivity and hardness measurements performed in a subsequent in situ heat treatments carried out in the temperature range −20 °C to 180 °C. The solid lines through the data points are curve fits.

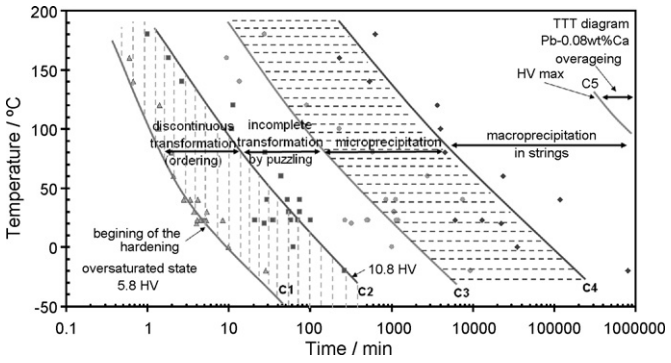

Fig. 11. TTT diagram for an alloy Pb–0.08 wt%Ca. Samples were cast, then cooled in liquid state at a minimum of 40 °C s^{-1} to −196 °C. Curves are obtained by resistivity and hardness measurements performed in a subsequent in situ heat treatments carried out in the temperature range −20 °C to 180 °C. The solid lines through the data points are curve fits.

This alloy has an intermediate behaviour between alloys with concentration of 600 and 1000 ppm (Fig. 11). For the alloys studied with calcium concentrations of 600, 1000, 1280 ppm, the points of the beginning and end of each transformation are perfectly reproducible and distinctive on the micro-hardness and resistance curves. As a consequence, the limit of the domains of transformations of the TTT diagrams (Figs. 4, 10 and 11) are constructed by lining up the points. For Pb–0.08 wt%Ca alloys the identification of the transformations borders are not as simple. The transformation overlapping is wider and consequently the deconvolution is more difficult. Curve C_1 is well defined (Fig. 11) because it is the first one, whereas the positions of the curves C_2–C_5 has required many more samples in order to be precisely defined.

3.2.3. Hyperperitectic compositions (1280 ppm Ca)

The alloy Pb–0.128 wt%Ca shows a hardness evolution that is completely different from the hypoperitectic compositions presented above. In Fig. 12, the alloy has already undergone a hardening transformation when the measurements begin at 20 °C. This level of hardness with transformations completed in the first minute of ageing is common for alloys with 800 wt ppm of calcium aged at 80 °C for example; but for Pb–0.128 wt%Ca, the transformation is probably complete because the hardness is nearly homogeneous in the sample during the first 40 min at 20 °C. The second hardening transformation appears after a long incubation

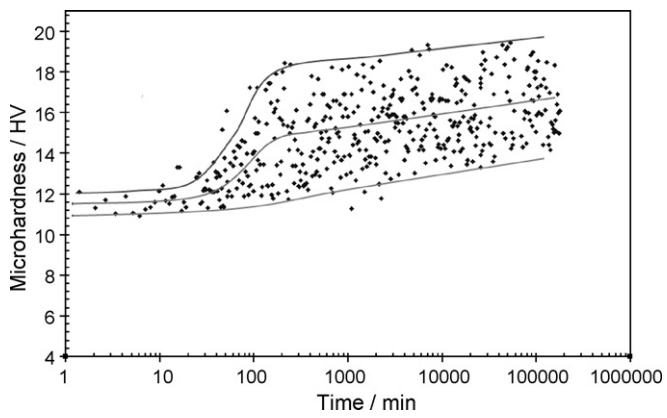

Fig. 12. Evolution of the micro-hardness on a Pb–0.128 wt%Ca alloy aged at 20 °C. The points correspond to hardness measurements $HV_{/0.1/5}$ on a single sample. As samples are inhomogeneous in hardness due to the presence of discontinuous transformations, fitted grey solid lines are added to represent the mean and the maximum, minimum curve to visualise the amplitude.

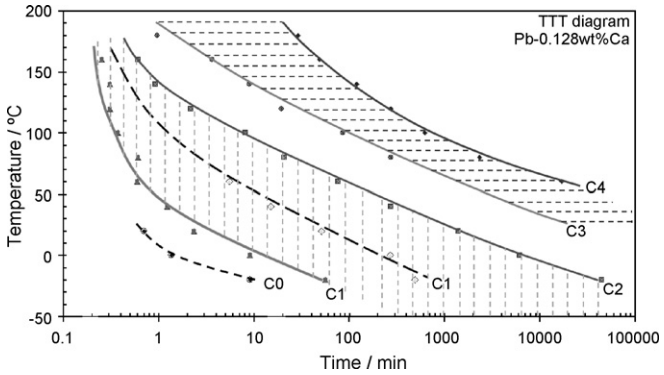

Fig. 13. TTT diagram for an alloy Pb–0.128 wt%Ca. Samples were cast, then cooled in liquid state at a minimum of 40 °C s^{-1} to −196 °C. Curves are obtained by resistivity and hardness measurements performed in a subsequent in situ heat treatments carried out in the temperature range −20 °C to 180 °C. The solid lines through the data points are curve fits.

and is characterised by a significant increase in the hardness values. The differences with the previous compositions presented may be explained by the fact that the composition is hyperperitectic. The transformation mechanisms must be quite different from for alloys with lower levels of calcium. The TTT diagram shown in Fig. 13, for a Pb–0.128 wt%Ca alloy, shows two new curves, C_0 and $C_{1'}$. These new frontiers correspond to the appearance of new inflexion points on the resistance curves and cannot be explained without microstructural analysis. Nanoscale observations with TEM will be needed to understand the transformation mechanisms for hyperperitectic compositions.

The TTT diagrams of hypoperitectic compositions show that the concentration of calcium has a major impact on the kinetics of the transformations. The effect of the concentration of calcium has been summarized in the TTT diagram in Fig. 13 with the superimposing of the limits for the three hypoperitectic compositions studied.

4. Conclusions

The construction of TTT diagrams with a wide range of concentration of calcium enables us to fully understand and overcome the transformation in lead–calcium alloys. It is now possible to predict the state of the alloy or determine the thermal cycle necessary to obtain a given microstructure. Nevertheless, the TTT diagrams shown are determined for parts produced with specific process parameters. Changing these conditions may change the kinetics and possibly the mechanism of the transformations.

References

[1] E.E. Schumacher, G.M. Bouton, Metals and Alloys 1 (1930) 405–409.
[2] D.E. Kelly, The influence of ternary additions on the kinetics of discontinuous precipitation of lead–calcium alloys, Ph.D. Thesis, University of Waterloo, Ont., Canada, 1985.
[3] H. Tsubakino, R. Nozato, Y. Satoh, Zeitschrift für Metallkunde 81 (1990) 490–495.
[4] J.P. Hilger, L. Bouirden, Journal of Alloys and Compounds 236 (1996) 224–228.
[5] H. Tsubakino, R. Nozato, A. Yamamoto, Scripta Metallurgica et Materialia 26 (1992) 1681–1685.
[6] H. Tsubakino, R. Nozato, A. Yamamoto, Zeitschrift für Metallkunde 84 (1993) 29–32.
[7] H. Tsubakino, M. Tagami, S. Ioku, A. Yamamoto, Metallurgical and Materials Transactions A: Physical Metallurgy and Materials Science 27 (1996) 1675–1682.
[8] G. Bourguignon, Amélioration du comportement électrochimique des batteries plomb-acide à usage photovoltaïque, Ph.D. Thesis, University of Nancy I, France, 2003.
[9] M. Dehmas, A. Maître, J.B. Richir, P. Archambault, Journal of Power Sources (2006).
[10] F. Rossi, Etude et comprehension des mécanismes de vieillissement des alliages de plomb-calcium, Ph.D. Thesis, Arts et Métiers ParisTech, Paris, France, 2006.
[11] W.A. Johnson, R.F. Mehl, Transaction of AIME 139 (1936) p416.
[12] Handbook of Chemistry and Physics, 70th edition, CRC Press, Cleveland, OH, 1989.
[13] M. Oberdorfer, F. Grass, Zeitschrift für Metallkunde 61 (1970) 458–461.